physica status solidi b
www.pss-b.com
basic solid state physics

Why are spin wave excitations all important in nanoscale magnetism?

Klaus Baberschke

Institut für Experimentalphysik, Freie Universität Berlin, Arnimallee 14, 14195 Berlin, Germany

Received 16 August 2007, revised 6 November 2007, accepted 23 November 2007
Published online 14 December 2007

PACS 75.30.Gw, 75.40.Gb, 75.75.+a, 76.50.+g

For a proper interpretation of magnetic phenomena in low dimensional magnets, higher order spin wave excitations are more important than in bulk magnetism. Three different types of experiments will be discussed: (i) In a so-called *trilayer*, two ferromagnetic films are coupled via a nonmagnetic spacer: FM1/NM/FM2. The individual Curie temperatures can be shifted by 50 K or 100 K, just by tuning the NM thickness. This is impossible in 3D. (ii) Spin-wave excitations are the major route to understanding the T-dependence of the interlayer exchange coupling (IEC). (iii) The standard Gilbert damping is insufficient to describe the spin dynamics in nanomagnets. Magnon–magnon scattering, a reversible process in the magnetic subsystem, must first be disentangled in the spin dynamics, before determining the dissipative relaxation into the thermal bath.

phys. stat. sol. (b) **245**, No. 1, 174–181 (2008) / **DOI** 10.1002/pssb.200776452

phys. stat. sol. (b) **245**, No. 1, 174–181 (2008) / **DOI** 10.1002/pssb.200776452

physica status solidi b
www.pss-b.com
basic solid state physics

Why are spin wave excitations all important in nanoscale magnetism?**

Klaus Baberschke*

Institut für Experimentalphysik, Freie Universität Berlin, Arnimallee 14, 14195 Berlin, Germany

Received 16 August 2007, revised 6 November 2007, accepted 23 November 2007
Published online 14 December 2007

PACS 75.30.Gw, 75.40.Gb, 75.75.+a, 76.50.+g

* e-mail bab@physik.fu-berlin.de
** This work was presented as an invited talk at the International Conference on Nanoscale Magnetism (ICNM-2007), 25–29 June 2007, in Istanbul.

For a proper interpretation of magnetic phenomena in low dimensional magnets, higher order spin wave excitations are more important than in bulk magnetism. Three different types of experiments will be discussed: (i) In a so-called *trilayer*, two ferromagnetic films are coupled via a nonmagnetic spacer: FM1/NM/FM2. The individual Curie temperatures can be shifted by 50 K or 100 K, just by tuning the NM thickness. This is impossible in 3D. (ii) Spin-wave excitations are the major route to understanding the T-dependence of the interlayer exchange coupling (IEC). (iii) The standard Gilbert damping is insufficient to describe the spin dynamics in nanomagnets. Magnon–magnon scattering, a reversible process in the magnetic subsystem, must first be disentangled in the spin dynamics, before determining the dissipative relaxation into the thermal bath.

1 Introduction Spin wave excitations and spin fluctuations (critical or Gaussian) are well established subjects in bulk magnetism and are summarized in several textbooks, e.g. in Ref. [1, 2]. Frequently, the theory of bulk ferromagnetism is used and applied to analyze and interpret the spin dynamics in nanomagnets, e.g. the standard Landau–Lifshitz equation of motion plus Gilbert damping (LLG), the static exchange field in multilayers, a $T = 0$ approach in theory, etc. On the other hand, it is well established that fluctuations become more important in one or two dimensional systems than in three dimensional bulk materials. In low dimensional magnets the spin fluctuations may become so dramatic that ferromagnetic ordering will not take place at finite temperatures – the well known *Mermin–Wagner* theorem. This will happen only in an ideal isotropic Heisenberg ferromagnet; fortunately all real ferromagnets possess some anisotropic field contributions and thus do order at finite temperatures. Even so, the spin fluctuations remain important; this reduces the critical temperature T_c below the bulk value if the three-dimensional magnet is reduced to a two-dimensional plate or a one-dimensional chain – the well known *finite size effect*. So the question arises: can one always interpret the magnetism of nanostructures within the framework of the theory for bulk magnetism i.e. in the molecular field picture or the Stoner model? The answer will be "no". Spin-wave excitations need to be given more weight than in 3D bulk magnetism.

The prototype of a magnetic multilayer structure is the so-called *trilayer*, depicted schematically in Fig. 1. Two ultrathin films are separated by a nonmagnetic spacer layer (NM). The ferromagnetic layers FM1 and FM2 will consist of only a few atomic layers (2–10 ML), having Curie temperatures and anisotropy fields which differ from those of the bulk material. The thickness of the spacer can be tuned in theory and experiment to give ferromagnetic or antiferromagnetic coupling between FM1 and FM2 and different strengths of the interlayer exchange coupling [3, 4]. In theory, such a system can be solved only in an approximate way, as indicated schematically in Eq. (1).

$$\frac{\partial}{\partial t}\langle\langle S_i^+; S_j^-\rangle\rangle \rightarrow S_i^z S_j^+ \approx \langle S_i^z\rangle S_j^+ - \langle S_i^- S_i^+\rangle S_j^+ - \langle S_i^- S_j^+\rangle S_i^+ + \ldots \quad (1)$$

To decouple the higher order Green's function in the equation of motion, products of operators, such as $S_i^z S_j^+$, are approximated by expectation values as indicated on the right-hand side of Eq. (1). For bulk magnetism, the first term, $\langle S_i^z\rangle S_j^+$ – i.e. the mean field approximation – is suf-

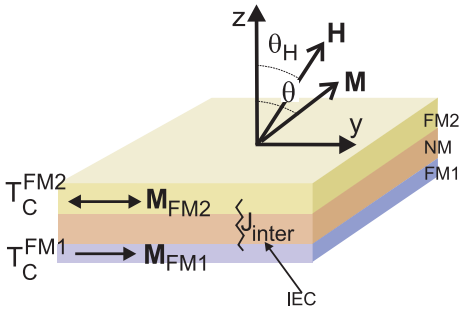

Figure 1 (online colour at: www.pss-b.com) Schematic illustration of the prototype trilayer.

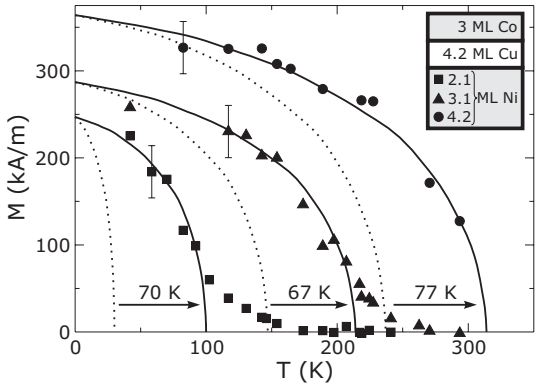

Figure 2 $M_{Ni}(T)$ in a trilayer (solid symbols) with a Ni staircase and constant d_{Cu} and d_{Co}. The dotted curves give the expected values for Cu-capped single Ni films with the same thickness. $M_{Co}(T)$ not shown, for details see [8–10].

ficient in most cases. Higher-order Green's functions are approximated by the Tyablikov (RPA) decoupling. This creates the second term in Eq. (1) with the off diagonal on-site term, $\langle S_i^- S_i^+ \rangle$. We will show in Section 2 that it is required to describe some of the magnetic features of two-dimensional magnets. Even the RPA may be insufficient to describe spin-wave excitations, and the third term, with off-site expectation values such as $\langle S_i^- S_j^+ \rangle$, is needed for the proper description of magnon–magnon scattering.

Three different types of our experiments are discussed, here. They have in common, that a mean field picture is insufficient to explain the experimental findings. In Section 2 X-ray magnetic circular dichroism (XMCD) is used to study the enormous shifts of the Curie temperatures in trilayers (Fig. 1). Section 3 focuses on the temperature dependence of the interlayer exchange coupling (IEC, Fig. 1). Mostly the electronic band structure in the $T = 0$ limit has been discussed; see e.g. Stiles in Ref. [5]. Here ferromagnetic resonance (FMR) measurements over the full T-range from $T \approx 0$ up to T_C will be analyzed. In Section 4 the linewidth of FMR is disentangled in (i) dissipative damping (Gilbert damping, Heinrich in Ref. [5]) and (ii) (elastic) scattering in the magnetic subsystem (e.g. magnon–magnon scattering). None of the three sections is intended to deliver a full overview in this field. For this we refer to the new five volumes of the Handbook of Magnetism [6]. Here, we focus only on a conceptual bridging between different experiments and the prominent role of magnon–magnon interactions.

2 Curie temperatures of ferromagnetic trilayers

One of the most instructive examples to demonstrate the importance of higher-order spin-spin correlations in low dimensional ferromagnets is the study of the temperature dependence of the magnetization of the layers FM1 and FM2 and their corresponding ordering temperatures in magnetic trilayers. Here we summarize the results.

Let us assume that the trilayer is composed of a Co ultrathin film on the top and a Ni ultrathin film on the bottom, separated by a Cu spacer (schematic inset in Fig. 2). XMCD is the technique of choice to study the element-specific magnetization. When tuning the synchrotron radiation to the L_3 edge of Ni, only $M(T)$ for Ni is detected, while tuning to the L_3 edge of Co gives $M(T)$ for Co alone. Details of the experimental study have been published elsewhere [7]. If such an experiment is performed *in situ* in UHV, one could evaporate and measure just the bottom Ni film (dotted line in Fig. 2), then add the spacer and Co films on top and measure the Ni magnetization again (solid line and experimental data points). We see that 2.1 ML of Ni have a T_C of approx 40 K, and that it is shifted by about 70 K to higher values with the spacer and Co film on top. At first glance one could argue that the exchange field from the Co layer on top will increase the Ni magnetization (field-induced magnetization). But it is easily seen that this is not a sufficient explanation. An additional magnetic field of several Tesla, be it externally applied or the exchange field of Co, will increase the magnetization of the FM1 film only by a few percent. But here, we observe a shift of 70 K and more, which when normalized to the T_C of the single film corresponds to 30 or even more than 100 percent. Also, for a thicker Ni of 3.1 ML, a shift from ~150 K to ~215 K is observed, corresponding to ~40 percent.

A much more realistic interpretation of this enormous shift of the critical temperature in a trilayer was given by Jensen [11]. He calculated $M(T)$ and the corresponding T_C of such a system in two ways: (i) using a Heisenberg Hamiltonian, he calculated only in the mean field (MF) approximation, corresponding to the first term in Eq. (1); (ii) he included in the same calculation also the second term in the above equation, the RPA. In both cases he took the same magnetic moment per Ni ion and chose the same coupling strength as shown to be 310 μeV, or a weaker coupling of 86 μeV. It becomes clear from Fig. 3 if only the static exchange field of the top Co film were acting (MF), that there would be a small increase of a few percent in the Curie temperature. If, however, we add also the off-diagonal terms (RPA) in the calculation, we find a large shift and increase of T_C, and this effect increases dramatically the thinner (more 2D-like) FM1 becomes. One might argue that the Heisenberg Hamiltonian is less appropriate to calculate the temperature dependence of the magnetiza-

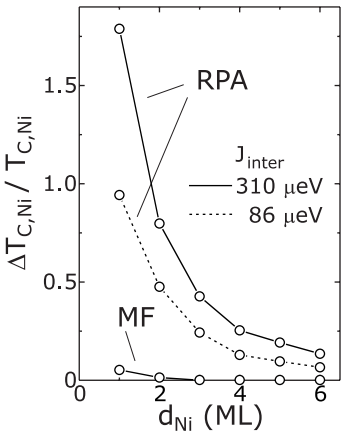

Figure 3 Enhancement of T_C in a trilayer as function of the film thickness. In MF only a small increase in T_C is calculated. Taking the same coupling parameters but adding the RPA contribution (see Eq. (1)) increases the enhancement dramatically; this becomes increasingly important, the thinner the film [11].

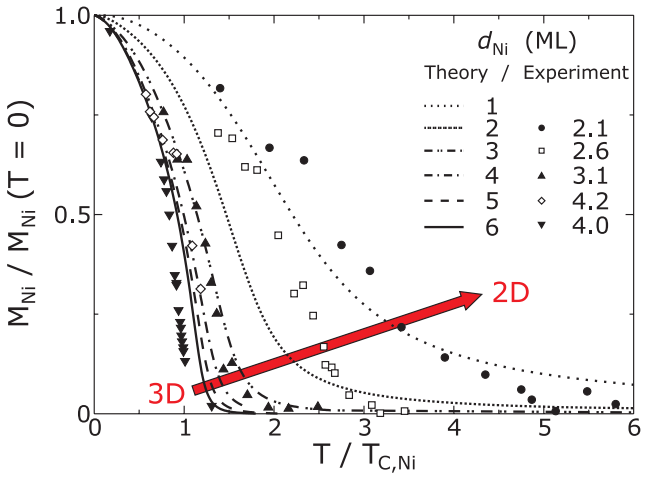

Figure 4 (online colour at: www.pss-b.com) Ni magnetization of a Co/Cu/Ni trilayer as a function of relative temperature. The Co and Cu thicknesses were kept constant. The experimental data for $d_{Ni} = 2.1$, 3.1 and 4.2 are the same as in Fig. 2. For the experiment with 4.0 ML $J_{inter} = 0$. For the calculation a constant $J_{inter} = 310$ μeV was taken [7].

tion of itinerant ferromagnets. Fortunately Nolting and coworkers have calculated $M(T)$ and the corresponding T_C of the same trilayer system using a Hubbard Hamiltonian. In Ref. [12], they report also very large shifts of 30 K or 60 K, depending on the individual parameters of the magnetic layers.

The importance of spin-spin correlations for 2D magnetism is again illustrated in Fig. 4. The relative Ni magnetization normalized to its $T = 0$ value for a Co/Cu/Ni trilayer is plotted as function of the reduced temperature. $M(T)$ vanishes at its Curie temperature T_C. The theory starts with a thick 6 ML Ni film and a Co film on top. In the further calculation, the Ni thickness is reduced layer-by-layer while everything else is kept constant. T_C and the tail of $M(T)$ increase dramatically. Note: The tail depends on the Ni thickness, not only on the exchange field of the top Co film, which is constant [7]. In the experiments, we could not prepare a monatomic layer, but varied the thickness of the Ni film between 2 ML and 4 ML. The same trend was verified. The thinner the film, the larger the tail above T_C. If only a static Co exchange field were acting on the Ni film, be it in theory or experiment, the tail of the magnetization should be independent of the layer thickness.

In conclusion: only higher order spin-spin correlations can explain the $M(T)$ and T_c behavior of ultrathin trilayers. Figure 4 shows clearly that the tail of the Ni magnetization increases dramatically as d_{Ni} becomes thinner, keeping d_{Co} and its exchange field constant.

These experiments initiated another type of discussion: Does a trilayer with two different ferromagnets have one or two values of T_C? One very canonical answer would be: just one Curie temperature, namely the higher T_C – in our case it is the T_C of Co. If so, one should call the lower T_C (in our case that of Ni) T_C^*. On the other hand, two maxima in the susceptibility have been observed, also. Recently Eriksson and coworkers have analyzed the spin-spin correlation function for a trilayer system similar to our experimental situation. They show that, indeed, two distinct temperatures can be identified [13].

3 Temperature dependence of interlayer exchange coupling The interlayer exchange coupling as indicated in Fig. 1 turns out to be one of the most important parameters for magnetic multilayers and nanostructured superlattices. The spacer layer in our work was copper; in general it could be of semiconducting or insulating spacer material as well, and even antiferromagnetic chromium has been used. The leading parameter which controls the sign and the strength of the IEC is determined by the electronic band structure of the NM spacer material. This is discussed in many review articles, e.g. see the chapters by Stiles in Ref. [5] and by Hathaway in Ref. [14]. For copper as spacer material the pioneering IEC calculations were presented by Bruno [3]. Many of the experimental and theoretical investigations dealt with spacer thicknesses $d > 1$ nm. Here, we concentrate on ultrathin spacers in the range of $d = 2$–6 ML. This gives us the flexibility to tune the strength and sign of the IEC over a wide range between weak and strong coupling (Fig. 5). For details see [15].

In 1995, two independent theoretical works appeared, focusing on the temperature dependence of the IEC, which turned out to be important when comparing theory with experimental data and technological applications at finite temperatures. Bruno and coauthors [3, 16] concentrated on the smearing of the Fermi edges at elevated temperatures as given by Eq. (2) with the controlling parameters T_0, the Fermi velocity v_F, and the thickness d. For more compli-

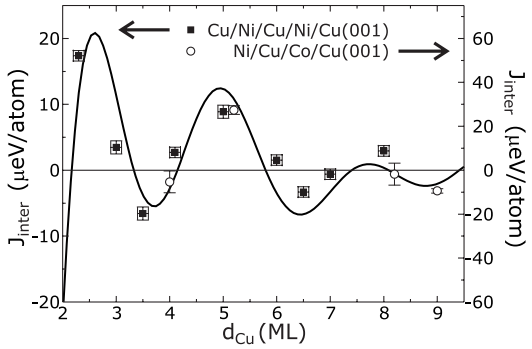

Figure 5 J_{inter} oscillations as function of the Cu spacer thickness of 2–9 ML. The absolute numbers of energy/atom were measured with UHV-FMR [4].

cated Fermi surfaces, one might also use the sum of several Fermi velocities.

$$J_{inter} = J_0 \frac{T/T_0}{\sinh(T/T_0)}, \quad T_0 = \hbar v_F / 2\pi k_B d\,. \tag{2}$$

Mills and coauthors focused on the spin excitation at finite temperatures in the films FM1 and FM2 [17]. There, the temperature dependence of the IEC follows a $T^{3/2}$ power law, as shown in the following equation:

$$J_{inter} = J_0[1 - (T/T_C)^{3/2}]\,. \tag{3}$$

In this equation the thickness of the spacer and other material parameters are hidden in the prefactor. This result shows explicitly the Curie temperature T_C at which ferromagnetism and the coupling vanishes. In the former equation, the FM ordering temperature T_C does not appear explicitly and is hidden in the prefactor.

The first experimental investigations to measure the IEC by means of temperature dependent FMR experiments were measured over a small temperature range [19, 20]. In a recent letter [21], three different systems, viz. Ni_9CuCo_2, Ni_8CuNi_9 trilayers, and a Fe_2/V_5 multilayer, have been investigated over a very large temperature range starting at nearly $T \approx 0$ and ranging up to T_C. The authors plotted the measured J_{inter} as function of reduced temperature $(T/T_C)^{3/2}$ (Eq. (3)) and it was evident that this dependence fits the experimental data better than the sinh function. The excitation of spin waves seems to be the dominant contribution of the T-dependence of the IEC. It could reduce the IEC down to 20–30 percent at ambient temperature. The temperature dependence in the band structure plays only a minor role [21]. Very recently, this problem has been taken up by Nolting and co-workers. They used a microscopic Heisenberg model to calculate the temperature dependence of low energy spin-wave excitations [18]. The difference in the free energy for parallel and antiparallel orientations of magnetization in the FM1 and FM2 layers contributes to the temperature dependence of the IEC parameter J_{inter}. This basically depends on two quantities: (i) the direct exchange coupling J_{intra} *within* the ferromagnetic layer, yielding also its Curie temperature, and (ii) the interlayer exchange coupling J_{inter} *between* the two layers FM1 and FM2. The direct exchange in each FM layer J_{intra} is much stronger, being in the meV regime, while the IEC coupling J_{inter} for weak coupling in trilayers with spacer thickness $d \approx 3$–9 ML is in the μeV range. To extract the effect of the magnetic contributions alone for different spacer thicknesses, J_{inter} has been normalized to the parameter $J_0 = J_{inter}(T = 0)$. Schwieger et al. [18] have discussed J_{inter}/J_0 in terms of an effective $T^{1.5}$ power law. It is important to note that $J_{inter}(T)$ also depends on the type of magnetic material used, which points up the competition between the thermal energy and the strength of the coupling. The T dependence of the normalized J_{inter} for different J_0 values was studied and it could be seen that effectively, a power law is obeyed. However, it was also clear that the results did not follow a straight line in $T^{1.5}$ (see Fig. 1–5 in Ref. [18]). The curvature and slope both depend on the parameters J_{intra} and J_0. It could be seen that the larger the J_0 value, the weaker the decrease of J_{inter} with T. *All* contributions due either to the

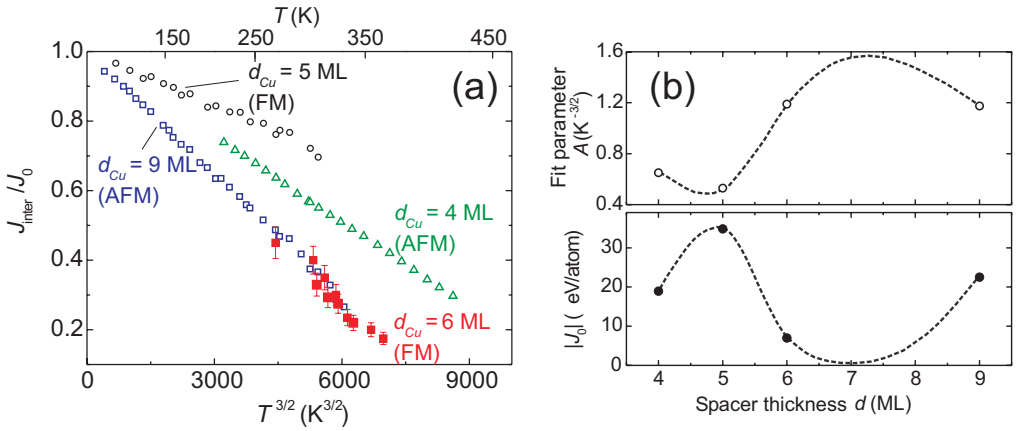

Figure 6 (online colour at: www.pss-b.com) (a) Normalized J_{inter} for a $Ni_7Cu_nCo_2$ trilayer and variable d_{Cu} measured with *in situ* UHV-FMR [24]. (b) Top: Fit parameter A vs. spacer thickness. Bottom: J_0 vs. spacer thickness (see Eq. (4)). The dashed curves are merely guides to the eye [24].

spacer, the interfaces, or the magnetic layers nevertheless do give an effective power law dependence on the temperature:

$$J(T) \approx 1 - AT^n, \quad n \approx 1.5 . \tag{4}$$

The differences between the above-mentioned mechanisms lie in their dependence on the spacer thickness. The spacer contribution, i.e. the electronic band structure effect, exhibits a linear dependence of A on d. The interface contribution is independent of d, while the contribution due to spin-wave excitation gives a very weak dependence and oscillates with d. It could be summarized that J_0 and the scaling parameter A should follow opposite trends as functions of spacer thickness [18]. This theoretical prediction was investigated recently using the *in situ* UHV-FMR technique. FMR offers the possibility to determine the values of J_{inter} in absolute energy units. The details of the experimental setup have been described elsewhere [15, 22]. Figure 6a shows the T-dependent IEC for different d_{Cu} with FM and AFM coupling (for details see [23, 24]). From these data, one could extract the parameter A in Eq. (4), and compare it with the J_0 value. This is shown in Fig. 6b, where it is clear that the scaling parameter A is neither independent nor a linear function of d, as would have been expected from a dominant interface effect or spacer electronic band-structure contribution. Instead, the oscillations in A give an experimental verification of the theory forwarded by Schwieger and Nolting [18]. It is a clear conclusion that the excitation of spin waves – or in other words, the creation of thermal magnons – is the dominant origin of the temperature dependence of J_{inter} in FM and AFM coupled trilayers.

4 Gilbert damping vs. spin wave excitations

In the following we focus on the analysis of the linewidth in FMR experiments in ultrathin films. This is of particular importance for the investigation of magnetization dynamics and magnetization reversal in nanostructures. Commonly, the ansatz is made of adding the so-called Gilbert damping to the equation of motion Eq. (5), i.e. the second term in Eq. (5). This Landau–Lifshitz–Gilbert equation (LLG) has been discussed in great detail in many review articles. For FMR on bulk material, see for example Ref. [2, 25]; for ultrathin films see Ref. [14, 26].

The Gilbert ansatz is based on a double vector product $-\boldsymbol{M} \times (\boldsymbol{M} \times \boldsymbol{H}_{\text{eff}})$ as shown in Figure 7b with a resultant vector pointing towards the symmetry axis of the Larmor precession. For small angles β between H_{eff} and M this can be approximated by the time derivative $\partial \boldsymbol{M}/\partial t$ (see [27] and standard textbooks):

$$\frac{\partial \boldsymbol{M}}{\partial t} = -\gamma(\boldsymbol{M} \times \boldsymbol{H}_{\text{eff}}) + \frac{G}{\gamma M_S^2}\left[\boldsymbol{M} \times \frac{\partial \boldsymbol{M}}{\partial t}\right] \tag{5}$$

and $\alpha = G/\gamma M$.

The viscosity damps the Larmor precession and the magnetization spirals into the z-axis, pointing to the surface of a sphere, i.e. the length of $\boldsymbol{M}$ stays constant but the expectation value $\langle M_z \rangle$ increases as the angle between the effective field and the magnetization $\beta \to 0$.

This is indicated in Fig. 7a as relaxation path 1. A uniform motion of the magnetization plus a viscous (Stokes) damping leads to a dissipation of energy into the thermal bath – an irreversible process. Two notations are commonly used in Eq. (5): (i) G, the Gilbert damping parameter, given as a relaxation rate in s^{-1}, or (ii) the dimensionless parameter α, in analogy to the viscous damping. The relaxation rate per second G seems to be more instructive for easier comparison with other relaxation rates in the literature. Standard EPR/FMR experiments use a fixed microwave frequency and scan the external Zeeman field H_0. Under these conditions, the LLG (5) leads to a linewidth ΔH_G depending linearly[1] on ω:

$$\Delta H_G(\omega) \approx \frac{2}{\sqrt{3}} \frac{G}{\gamma^2 M} \frac{\omega}{\cos\beta} . \tag{6}$$

A second relaxation process is discussed in the standard literature and indicated in Fig. 7c: The uniform motion of the magnetization may scatter into excited states of the magnetic subsystem (spin waves, Stoner excitations, magnon–magnon scattering etc.) The projection of $\boldsymbol{M}$ onto the z-axis stays constant since the precessional energy is scattered into the transverse components M_x and M_y, as indicated in Fig. 7c. For details see [1, 2]. These processes may be reversible and are indicated in Fig. 7a as path 2. In the long run these excitations will also decay into the thermal bath as indicated by path 3. One may raise the question: Is there any experimental evidence for the appearance of this second relaxation process, i.e. scattering within the magnetic subsystem, in magnetic nanostructures? In other words: Should one always take the experimental linewidth and label it with a phenomenological Gilbert parameter (following Eq. (6)), or is it possible to separate first the scattering within the magnetic subsystem from the dissipative relaxation to the thermal bath. The theoretical background to study this question has been known for a long time. One possible model is described by the Bloch–Bloembergen equation [28, 29]

$$\frac{\partial \boldsymbol{M}}{\partial t} = -\gamma(\boldsymbol{M} \times \boldsymbol{H}_{\text{eff}}) - \frac{M_x}{T_2}\hat{e}_x - \frac{M_y}{T_2}\hat{e}_y - \frac{M_z - M_S}{T_1}\hat{e}_z . \tag{7}$$

[1] Note that this linear frequency dependence is a consequence of the field scanning technique in conventional FMR. For other experimental techniques at fixed magnetic field with scanning of the microwave frequency, or for Brillouin light scattering, the analysis of the measured linewidth is different; see [26]. Caution has to be taken when comparing different experiments.

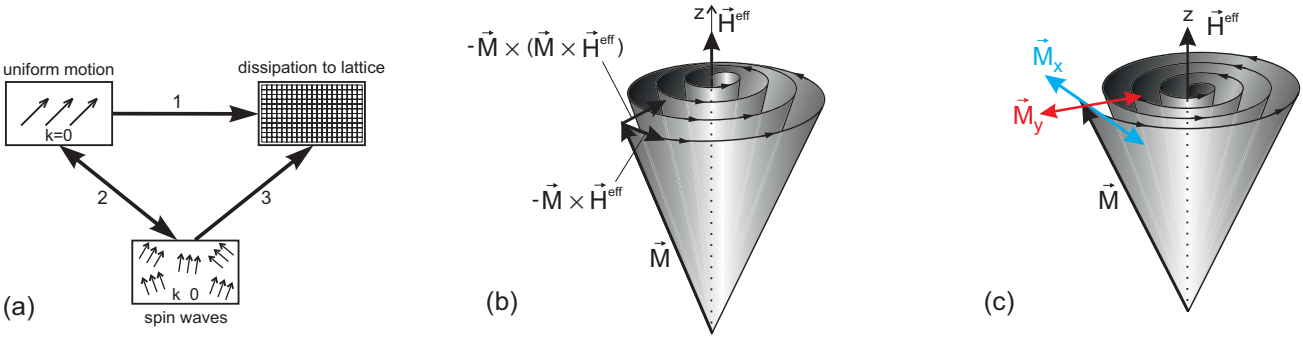

Figure 7 (online colour at: www.pss-b.com) Schematic illustration of different relaxation processes taken from [2, 31]: (a) The uniform motion of the magnetization with $k = 0$ in an FMR experiment may scatter with energy dissipation into the thermal bath (path 1). In path 2, it can also scatter into spin waves with $k \neq 0$ – a reversible process. At the long run this energy travels also along path 3 into the heat sink. (b) depicts the LLG scenario from Eq. (5). (c) shows the Bloch–Bloembergen process for spin–spin relaxation.

In this case, two different relaxation times are introduced into the equation of motion [30]: the longitudinal relaxation time T_1, i.e. the direct path into the thermal bath, and the so-called transverse time, T_2, by which energy is scattered into the transverse magnetization components M_x and M_y. It is depicted in Fig. 7c. This describes a dephasing of the formerly coherent rotation of the magnetization. This scenario of a transverse relaxation rate is known, e.g. [2, 26, 31]. Recently, Arias and Mills have calculated this type of magnon-magnon scattering in a quantitative manner applied to standard FMR experiments in ultrathin films [32, 33]. The result for the FMR linewidth is given below:

$$\Delta H_{2M}(\omega) = \Gamma \sin^{-1}\sqrt{\frac{\sqrt{\omega^2 + (\omega_0/2)^2} - \omega_0/2}{\sqrt{\omega^2 + (\omega_0/2)^2} + \omega_0/2}}\,. \qquad (8)$$

It is obvious that the frequency dependence of the linewidth for magnon–magnon scattering is by no means linear. It saturates at very high frequencies and starts with a steep slope at low frequencies (Fig. 8). Surprisingly enough, FMR experimentalists have never tried to disentangle these different types of frequency dependence in a quantitative manner; most of them analyzed the experimental data in the frame of the LLG equation and linear ω dependence. In a plot of ΔH versus frequency, this leads in most cases to an apparent "residual" linewidth ΔH_0^* (see Fig. 8). In some cases, a non-linear dependence was observed, but the curved line was given only as a guide to the eye [34].

The first quantitative analysis of a nonlinear $\Delta H(\omega)$, following Eq. (8), was reported for Fe/V superlattices in [35]. Recently this has been extended to a very large frequency range from 1 GHz to 225 GHz as shown in Fig. 8 [36]. In this work, the authors also reanalyzed the data from [34] using Eq. (8) together with Eq. (6).

Several key pieces of information can be concluded from Fig. 8: (i) FMR measurements at very low frequencies (1–4 GHz) unambiguously show that the linewidth-narrows dramatically, that is to say ΔH is given by relaxation processes only, and no leftover inhomogeneous width at $\omega = 0$ is seen. It was a common practice in the literature for earlier experiments between 9 GHz and 36 GHz to *assume* a linear frequency dependence [14, 41] and extrapolate from this an apparent residual linewidth (the tangent-crossing the y-axis) ΔH_0^*. This procedure may be misleading

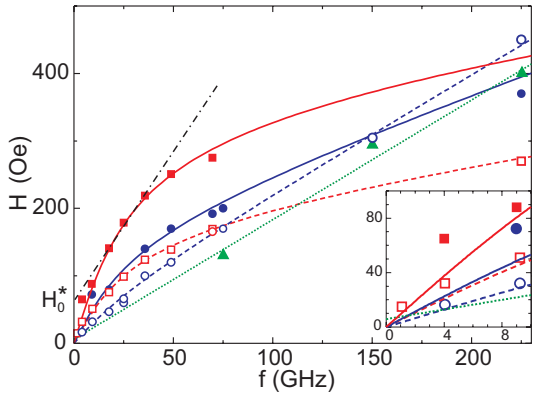

	G ($10^8 s^{-1}$)	G ($10^8 s^{-1}$)	H_0 (10^{-3})	H_0 (Oe)
■ Fe_4/V_2 ; H||[100]	51.9	0.20	0.97	0
● Fe_4/V_4 ; H||[100]	26.1	0.45	2.59	0
□ Fe_4/V_2 ; H||[110]	27.9	0.22	1.06	0
○ Fe_4/V_4 ; H||[110]	8.4	0.77	4.44	0
● Fe_4/V_4 ; H||[001]	0	0.76	4.38	5.8

Figure 8 (online colour at: www.pss-b.com) FMR linewidths of two Fe/V-multilayer samples for different in-plane and out-of-plane orientations of the external field as a function of the microwave frequency. The inset shows a magnified view of the low frequency regime. The table on the right lists the fit parameters corresponding to Eqs. (6) and (8). For details see [36].

ing [26] for a fundamental understanding of future experiments. (ii) For all in-plane orientations of the external field ([100] and [110]), one observes a nonlinear frequency dependence. In contrast, for $\boldsymbol{H}$ normal to the film plane ([001], full triangles) a 100% linear frequency dependence is observed. This is in perfect agreement with the theoretical prediction in [32, 33]. The authors of [36] deduce for the Fe_4/V_4 sample an almost constant (independent of orientation) Gilbert damping of $\sim 0.6 \times 10^8$ s^{-1}, but an angular dependence in the magnon–magnon scattering by more than a factor of 3 (first column in Fig. 8). For the Fe_4/V_2 sample, a two times smaller Gilbert damping of $\sim 0.2 \times 10^8$ s^{-1} is measured, but again the magnon–magnon scattering is about $10-25$ times faster. (iii) The angular dependence of the magnon–magnon scattering was independently confirmed by angular-dependent measurements (see [36]). Note: The anisotropic linewidth is caused by the magnon–magnon scattering; the Gilbert damping is more or less isotropic. (iv) Fitting Eq. (8) to the nonlinear frequency dependence yields a magnon–magnon scattering rate of $\gamma\Gamma \approx 10-50$ times larger than the Gilbert damping. Thus, experimental evidence is found that both relaxation mechanisms (longitudinal and transverse scattering) are active in magnetic nanostructures. A combination of magnon-magnon scattering, modelled by Eqs. (7) and (8), and a viscous Gilbert damping described by Eqs. (5) and (6) seems to give a better insight into the spin dynamics of ultrathin films. We suggest that as long as there is no better analytical expression given by theory, Eq. (8) be used to test the frequency dependence of measured FMR linewidths. For the particular systems investigated, Fe/V multilayers and Fe films on GaAs, the magnon–magnon scattering of $1/T_2 \approx 10^9$ s^{-1} is about two orders of magnitude faster than the viscous Gilbert damping of $1/T_1 \approx 10^7$ s^{-1}.

This approach has recently been used to study the spin dynamics in Fe_3Si binary Heusler-alloy thin structures epitaxially grown on MgO [37]. The authors performed angular-dependent measurements at 9.9 GHz and 24 GHz and frequency-dependent FMR experiments from 1 GHz to 70 GHz. They analyzed all data in one unique fitting procedure, including magnon–magnon scattering as well as Gilbert damping. The outcome yields an isotropic viscous Gilbert damping, all anisotropic features in the linewidth could be explained in terms of anisotropic spin wave excitations. The latter being 5 to 10 times faster. This is in accordance with standard textbook reasoning, that the scattering within the magnetic subsystem usually is faster than the energy dissipation. Finally we should mention that also other cases are known with linear frequency dependence over a large range, e.g. from 2 GHz to 16 GHz, see [42].

5 Summary All three types of experiments described above demonstrate the importance of higher-order spin-spin correlations in low dimensional magnetism. Such large shifts of T_C and increase of $M(T)$ in a trilayer (Section 2) "do not exist in 3D systems but only in systems with reduced dimensionality" (p. 503 in [38]). For the same reason thermal magnons play the dominant role in the T-dependence of the IEC (Section 3) – band structure effects play only a minor role. Recently the question was raised, "Is the LLG phenomenology applicable" in ultrathin films [39]? The answer in Section 4 will be, "No"! Advanced experiments and analysis allow – at least in part – the separation of magnon-magnon scattering from Gilbert viscous damping. Both scattering rates, when separated, will provide us with direct detailed insights into the spin dynamics. A "shake-up" in the magnetic subsystem occurs first and is 10 to 100 times faster than the energy dissipation path. From Section 4 and [36, 37] it becomes evident that the major fraction of anisotropy in the total relaxation rate is caused by the fast magnon-magnon scattering (Eqs. (7, 8)) in ultrathin films and only a minor contribution may come from the Gilbert damping (Eqs. (5, 6)).

Other routes have been followed to study the spin dynamics: e.g. the Gilbert constant α (Eq. (5)) has been assumed not to be constant, but rather an unspecified function $\alpha(\omega)$ [40]. Or α was kept constant and the FMR linewidth was postulated to be a linear function of ω (Eq. (5)), consequently an apparent residual width ΔH_0^* appeared [14, 41]. Moreover, anisotropic Gilbert damping has been postulated to be due to anisotropic conductivity and resistivity contributions. All these different types of phenomenological approaches in the analysis of spin dynamics on a microscopic scale do not disentangle excitations within the magnetic subsystem from energy dissipation into the thermal bath. This latter ansatz appears very transparent and seems to explain some experimental findings very naturally.

Acknowledgements Ongoing discussions with W. Nolting, D. L. Mills, W. D. Brewer, and P. J. Jensen are acknowledged. Special thanks go to my former coworkers, in particular for the assistance from S. S. Kalarickal, K. Lenz, and E. Kosubek.

References

[1] A. G. Gurevich and G. A. Melkov, Magnetic Oscillations and Waves (CRC Press, Boca Raton, 1996).
[2] M. Sparks, Ferromagnetic-Relaxation Theory (McGraw-Hill, New York, 1964).
[3] P. Bruno, Phys. Rev. B **52**, 411 (1995).
[4] J. Lindner and K. Baberschke, J. Phys.: Condens. Matter **15**, S465 (2003).
[5] J. A. C. Bland and B. Heinrich (eds.), Ultrathin Magnetic Structures III (Springer-Verlag, Berlin, 2005).
[6] H. Kronmüller and S. S. Parkin (eds.), Handbook of Magnetism and Advanced Magnetic Materials (John Wiley & Sons, New York, 2007).
[7] A. Scherz, C. Sorg, M. Bernien, N. Ponpandian, K. Baberschke, H. Wende, and P. J. Jensen, Phys. Rev. B **72**, 54447 (2005).
[8] U. Bovensiepen, F. Wilhelm, P. Srivastava, P. Poulopoulos, M. Farle, A. Ney, and K. Baberschke, Phys. Rev. Lett. **81**, 2368 (1998).

[9] U. Bovensiepen, F. Wilhelm, P. Srivastava, P. Poulopoulos, M. Farle, and K. Baberschke, phys. stat. sol. (a) **173**, 153 (1999).
[10] K. Baberschke, J. Magn. Magn. Mater. **272–276**, 1130 (2004).
[11] P. J. Jensen, K. H. Bennemann, P. Poulopoulos, M. Farle, F. Wilhelm, and K. Baberschke, Phys. Rev. B **60**, R14994 (1999).
[12] J. H. Wu, T. Potthoff, and W. Nolting, J. Phys.: Condens. Matter **12**, 2847 (2000).
[13] L. Bergqvist and O. Eriksson, J. Phys.: Condens. Matter **18**, 4853 (2006).
[14] B. Heinrich and J. A. C. Bland (eds.), Ultrathin Magnetic Structures II (Springer-Verlag, Berlin, 1994).
[15] J. Lindner and K. Baberschke, J. Phys.: Condens. Matter **15**, R193 (2003).
[16] V. Drchal, J. Kudrnovsky, P. Bruno, I. Turek, P. H. Dederichs, and P. Weinberger, Phys. Rev. B **60**, 9588 (1999).
[17] N. S. Almeida, D. L. Mills, and M. Teitelmann, Phys. Rev. Lett. **75**, 733 (1995).
[18] S. Schwieger and W. Nolting, Phys. Rev. B **69**, 224413 (2004).
[19] Z. Zhang, L. Zhou, P. E. Wigen, and K. Ounadjela, Phys. Rev. Lett. **73**, 336 (1994).
[20] Z. Celinski, B. Heinrich, and J. F. Cochran, J. Magn. Magn. Mater. **145**, L1 (1995).
[21] J. Lindner, C. Rüdt, E. Kosubek, P. Poulopoulos, K. Baberschke, P. Blomquist, R. Wäppling, and D. L. Mills, Phys. Rev. Lett. **88**, 167206 (2002).
[22] K. Lenz, E. Kosubek, T. Tolinski, J. Lindner, and K. Baberschke, J. Phys.: Condens. Matter **15**, 7175 (2003).
[23] S. Schwieger, J. Kienert, K. Lenz, J. Lindner, K. Baberschke, and W. Nolting, Phys. Rev. Lett. **98**, 057205 (2007).
[24] S. S. Kalarickal, X. Y. Xu, K. Lenz, W. Kuch, and K. Baberschke, Phys. Rev. B **75**, 224429 (2007).
[25] S. V. Vonsovskii (ed.), Ferromagnetic Resonance (Pergamon Press, Oxford, London, 1966).
[26] D. L. Mills and S. M. Rezende, in: Spin Dynamics in Confined Magnetic Structure II, edited by B. Hillebrands and K. Ounadjela (Springer, Berlin, 2003).
[27] T. L. Gilbert, Ph.D. dissertation, Illinois Institute of Technology (1956).
T. Gilbert, IEEE Trans. Magn. **40**, 3443 (2004).
[28] N. Bloembergen, Phys. Rev. **78**, 572 (1950).
[29] F. Bloch, Phys. Rev. **70**, 460 (1946).
[30] A. Abragam and B. Bleaney, in: Electron Paramagnetic Resonance of Transition Ions, edited by W. Marshall and D. H. Wilkinson (Clarendon Press, Oxford, 1970).
[31] H. Suhl, IEEE Trans. Magn. **34**, 1834 (1998).
[32] R. Arias and D. L. Mills, Phys. Rev. B **60**, 7395 (1999).
[33] R. Arias and D. L. Mills, J. Appl. Phys. **87**, 5455 (2000).
[34] G. Woltersdorf and B. Heinrich, Phys. Rev. B **69**, 184417 (2004).
[35] J. Lindner, K. Lenz, E. Kosubek, K. Baberschke, D. Spoddig, R. Meckenstock, J. Pelzl, Z. Frait, and D. L. Mills, Phys. Rev. B **68**, 060102(R) (2003).
[36] K. Lenz, H. Wende, W. Kuch, K. Baberschke, K. Nagy, and A. Janossy, Phys. Rev. B **73**, 144424 (2006).
[37] Kh. Zakeri, J. Lindner, I. Barsukov, R. Meckenstock, M. Farle, U. von Hoersten, H. Wende, W. Keune, J. Rocker, S. S. Kalarickal, K. Lenz, W. Kuch, K. Baberschke, and Z. Frait, Phys. Rev. B **76**, 104416 (2007).
[38] J. Stöhr and H. C. Siegmann, Magnetism (Springer-Verlag, Berlin, Heidelberg, 2006).
[39] D. L. Mills and R. Arias, Physica B **284**, 147 (2006).
[40] G. Woltersdorf, M. Buess, B. Heinrich, and C. H. Back, Phys. Rev. Lett. **95**, 037401 (2005).
[41] Z. Celinsky and B. Heinrich, J. Appl. Phys. **70**, 5935 (1991).
[42] D. J. Twisselmann and R. D. McMichael, J. Appl. Phys. **93**, 6903 (2003).